AN AUSTRALIA–WIDE MAP OF CORROSIVITY: A GIS APPROACH

Australia-wide map of corrosivity

I.S. COLE, G.A. KING, G.S. TRINIDAD, W.Y. CHAN and
D.A. PATERSON
CSIRO Building, Construction and Engineering, Melbourne, Australia

Durability of Building Materials and Components 8. (1999) *Edited by M.A. Lacasse and D.J. Vanier*. Institute for Research in Construction, Ottawa ON, K1A 0R6, Canada, pp. 901-911.

Abstract

This paper presents two approaches to modelling atmospheric corrosion across regions of Australia. One is based on a purely statistical analysis of a large database of corrosion rates and climate. The other is based on combining such a statistical approach with modelling the sources and distribution of airborne salinity. The statistical approach is applied to data derived from a corrosivity survey of the State of South Australia. In this survey, corrosion rates were measured over 475 sites scattered over 420,000 km^2. The corrosion data was combined with climatic data and a model developed by regression analysis. This model proved highly accurate at describing the variation in corrosion rate across the state. Unfortunately, when the model was used to estimate corrosion rates across the Australian continent it proved highly inaccurate. As a response, a second model was developed. In this model, the role of the sea as a source of airborne salinity was explicitly included as were the factors (including wind direction) controlling the distribution of airborne salinity across the continent. This model was found to have reasonable accuracy, although additional factors (notably the effect of industrial pollution) still need to be incorporated.

Keywords: Atmospheric corrosion, mild steel, airborne salinity, sea state, whitecaps, wind direction, regression analysis

1 Introduction

Many authors have conducted exposure programs in which climatic parameters are monitored and statistical procedures (usually regression analysis) are used to derive relationships between the measured corrosion rates and the climatic parameters (Atteraas and Haagenrud 1982; Haynie 1982; Benarie and Lipfert 1986; Spence and Haynie 1990). Unfortunately, despite the detailed work carried out in this area and the many models proposed the scientific community has accepted no uniform model. In this paper, a model is derived from the combined analysis (multiple regression) of the results of an extensive corrosivity survey of South Australia and climatic data. It will be shown that this model can comprehensively account for the variation observed in the corrosion rate of the exposed plates. However, when the same model was applied to data from the whole of the Australian continent, it failed dramatically. This failure was instructive in a number of ways. Firstly, it underlined the limitations of models derived from "limited" data sets. In fact, the South Australian data set was the most extensive and reliable ever derived in Australia and in its scope exceeded that of the major European and American programs. However, the model contained intrinsic assumptions regarding a number of key characteristics of the climatic (including wind) patterns and pollutant patterns which, although valid for South Australia, were not valid for the rest of the continent. The key point is that a statistical model can only incorporate sources of variation that are relevant for the data set analysed. The converse is that climatic factors that can cause variations in zones outside the data set, if constant in the analysed data, will not occur in the models.

Given these limitations of statistically derived models, an attempt was made to develop a model more firmly based on understanding the processes controlling corrosion. In fact, the processes controlling corrosion across a continent are complex and it proved impossible to develop a pure process-based model. Thus, this paper presents a composite model where, although the generalised formulation may be based on an understanding of processes, many of the details of the model are derived from empirical methods or from fitting procedures (such as regression). The development of this model has been very informative in defining factors that may control the extent of corrosion across Australia.

2 A model of South Australian corrosivity

An initial corrosivity model for the State of South Australia was derived from statistical analysis.

2.1 The South Australian data set

South Australia is a southern/central sate of Australia, located between the latitudes of 38° and 26° south and the longitudes of 141° and 129°. The south-east of the State is moderately populated and has a temperate climate, while the majority of the rest of the state is semi-arid or arid. From 1991 to 1993, a corrosivity study was conducted over the whole state (420,000 km^2) using 475 sites. The site density varied considerably with the vast majority of sites in the coastal regions. At each site, duplicates of a low-alloy copper-bearing mild steel (BISRA) were exposed on brackets fixed to low voltage electric power supply poles at a height of 3.7 m above the ground and facing north. Corrosion rates over periods of one or two years were determined, however only the two-year data (in micron/year) is analysed in developing the models. Full details of procedures are given by King (1993).

2.2 The South Australian model

The model is based on regression analysis of measured corrosion rate as a function of a range of climatic and pollutant parameters. However, during the corrosivity survey, climatic data was not measured at the sites and thus a data set must be constructed. Site climatic data can be derived from data from meteorological stations using a triangular irregular network, or TIN, model (following the procedures of Okabe et al. (1992)). In addition to meteorological data, data on solar radiation was also derived following these procedures. The climatic and pollutant parameters included in the regression modelling are: solar radiation, average 3 pm RH (RH_{3pm}), average 9 am RH (RH_{9am}), average daily maximum temperature ($Temp_{max}$), average daily minimum temperature, mean temperature, rainfall (mm), and raindays.

In addition, each point is assigned an airborne salinity value. This salinity value is estimated using a simple model. This model makes the following assumptions:

- The salinity at the coast depends on the type of coast.
- A short-range (SRS) and a long-range (LRS) term can model the decrease in airborne salinity with increasing distance from the coast.
- Both of these terms show an inverse exponential decrease with distance from the coast.
- The rate at which the salinity falls off depends on the type of coast.

Formally the salinity factor (Sal) is defined as:

$$Sal = [LRS + (SRS \times s)]/(s + 1) \qquad \textbf{(1)}$$

where s is an integer defined by the coast type, and the units of salinity are mg/m^2.day. The values of s for different definitions of coast type, along with E, are given in Table 1. E in Eqs (2) and (3) is a measure of the salinity at the coast.

Table 1: Parameters for salinity at different coast types

Coast type	s	E
Very sheltered bay	1	5
Partially closed bay	2	15
Sheltered surf or very open bay	3	45
Open surf	4	130

LRS and SRS are then defined as:

$$LRS = E \times \exp[-dist \times (s + 1.5)/275] \qquad \textbf{(2)}$$

$$SRS = E \times \exp(-dist/\sqrt{s}) \qquad \textbf{(3)}$$

In these equations, dist is the minimum distance from the point to the nearest coast in an “allowable” direction. An allowable direction is one in which wind is observed to originate for at least 5% of the year.

These equations formalise the assumptions listed above. The separation of coast into different types and the assumption that there are long-range and short-range salt distribution terms is based on both measurements of airborne salinity (Cole and Ganther 1996) and on studies of salt production and wave mechanics. The values used for the initial airborne salinity is again based on actual measurements, however the exact formulation of rate of decrease and form of the decrease has been derived as a result of optimising the fit of the experimental data points.

When the salinity factor is included with the climate data, multiple regression yields the following approximations:

$$\mathrm{Ln(Corrosion)} = A \times \mathrm{Ln}(RH_{9am}) + B \times \mathrm{Ln}(Temp_{max}) + C \times \mathrm{Ln(Sal)} \quad \mathbf{(4)}$$

where A, B and C are constants derived from the regression analysis.

The mean average error of the model fit with the data is 0.143, which when converted from log gives an error of 15%. All the variables are significant at the 99% confidence level; the accuracy of the model (using Eq. (4)) is represented graphically in Figure. 1 which is a misfit diagram for South Australia. This diagram presents the predicted/measured corrosion rates. It is apparent that 80% of the predictions are within 20% of the measured data, and 97% of the predictions within 40% of the measured data. The above model assumes no effect of terrain. Variables were introduced into the regression analysis to test the sensitivity of the data to terrain factors. Variables included are elevation at site, highest elevation between the site and nearest coast, and the ratio of the last two variables. None of these variables increased the fit of the model in a significant way.

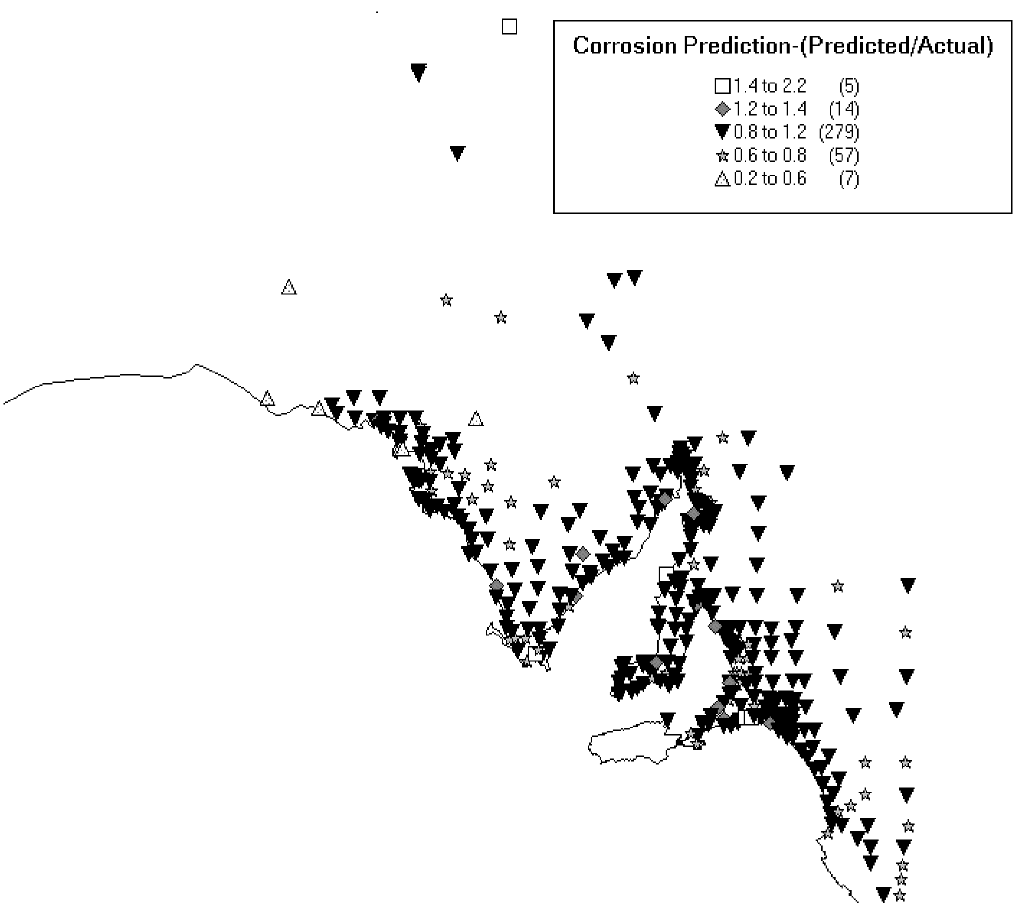

Fig. 1: Misfit diagram for South Australia

3 Application of the South Australian model to the continent

A data set of the corrosion rate of copper-containing mild steel was derived from a variety of published and unpublished data (Egan 1971; Martin 1973; Martin and King 1981; Smith et al. 1994). This data set contained 75 measurements in all Australian climatic zones. The South Australian model was applied to the Australian data set. A misfit diagram is given in Figure 2. The fit is extremely poor with over 41% of predictions being a factor of 2 greater than measured. Further, the model is extremely unreliable along the north-west coast of Australia.

4 Assumptions within the South Australian model

South Australia lies just above the latitude known as the "roaring forties" which is subject to strong westerly winds. The Great Australian Bight lies south of South Australia and is contiguous with the Southern Ocean. The bight is subject to high seas and the exposed coast of South Australia to significant surf. Further, the wind patterns across South Australia are relatively constant, with dominant westerlies shifting to south-westerlies and, in inland regions, to north-westerlies. Thus, for South Australia it is reasonable to assume that for a given beach type, airborne salinity is constant (that is the ocean state around the coast is constant) and that detailed modelling of wind direction is not required. These assumptions are invalid when applied to the Australian continent, as sea activity generally decreases further north while the weather patterns on the west and east coast of Australia are very variable and seasonal.

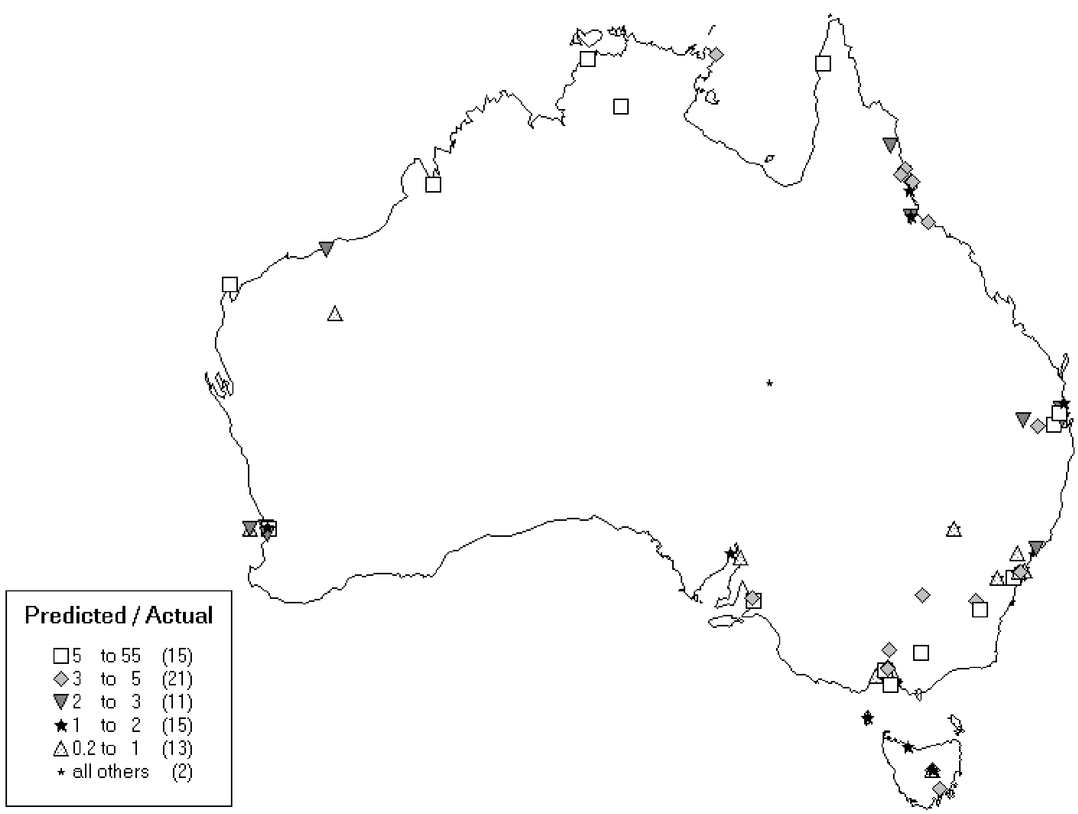

Fig. 2: Misfit diagram for South Australian model applied to Australia

5 The Australian model

The failure of the South Australian model when applied to Australia necessitated the development of a new Australian model. In this model, the effect of salinity sources and the effect of wind on salinity distribution are included explicitly in the model.

5.1 Basic formulation

The model maintains the partition of pollutant and climate effects, and is of the form:

$$\text{Corr} = A \times (\text{Sal})^B \times C \times (\text{Climate})^D \qquad \textbf{(5)}$$

The climate factor may be replaced by time of wetness.

5.2 Effect Of climate

Two climate models are proposed:

$$\text{Climate} = E \times RH_{3pm}{}^F \times \text{Raindays}^G \qquad \textbf{(6)}$$

$$\text{Climate} = H \times (\text{TOW-ISO})^I \qquad \textbf{(7)}$$

where TOW-ISO is time of wetness defined by the ISO Standard 9223, i.e. the surface is wet if RH is >80% and temperature is >0^{o}C. This condition is applied to three-hourly data on RH and temperature derived from ten years of meteorological data following the procedures outlined in the South Australian model.

5.3 Salinity

5.3.1 Sources of salinity

Studies of wave activity and airborne salinity over oceans indicate that relationships exist between sea state and salt production on the one hand, and sea state and latitude on the other. Salt aerosols may be generated either by the ocean or from surf, through bursting of bubbles generated by ocean whitecaps, particles torn from the crests of ocean whitecaps by the winds, and breakers on the shore.

An estimate of the sodium (and thus chloride) concentration in the air above the surf zone (Na_{surf}) can be given by (McKay et al. 1994):

$$Na_{surf} = e^{(0.23U - 16.72)} \qquad \textbf{(8)}$$

where U is the wind speed at 2 m above sea level (ms^{-1}).

Monahan (1980) demonstrated that the production of aerosol by the bursting of bubbles generated by whitecaps (dF_o/dr) is given by:

$$dF_o/dr = W\tau^{-1}\, dE/dr \qquad \textbf{(9)}$$

where r is aerosol radius, W is instantaneous fraction of the sea surface covered by whitecaps, τ is the time constant characterising the exponential whitecap decay (measured in seconds), and dE/dr is the differential whitecap aerosol productivity, i.e. the number of droplets per increment droplet radius produced by the decay of a unit area of whitecap.

However, Monahan et al. (1982) found that Eq. (9) could be approximated by:

$$dF_o = 1.373U^{3.41}\, r^{-3} \times 10^{1.19e^{-B^2}} \qquad \textbf{(10)}$$

where B = (0.380 – logr)/0.650.

Monahan et al. (1986) found that aerosol is also produced from spume drops that form as the result of mechanical disruption of wave crests by the wind. This mechanism becomes particularly effective at higher wind speeds and can be approximated by:

$$dF_1/dr = 6.45 \times 10^{-4}\, e^{2.08v}\, r^{-3}\, e^{-D^2} \qquad \textbf{(11)}$$

where D = 2.18 (1.88 – logr).

Total aerosol production is then given by:

$$DF/dr = dF_o/dr + dF_1/dr \qquad \textbf{(12)}$$

To derive salt production, it is also necessary to know the relationship between whitecap coverage and air speed which, according to Monahan et al. (1982), is given by:

$$W = 3.84 \times 10^{-6}\, U^{3.41} \qquad \textbf{(13)}$$

The monthly distribution of whitecaps around the globe has been derived from satellite observation (Monahan et al. 1982). From such data, the average whitecap coverage in the ocean adjacent to the coast has been determined. Using Eqs (10)–(13), the salt production at any point of the coast due to ocean activity can be approximated. From Eq. (9) the salt production from breaking surf can be estimated.

The salinity concentration at the coast is dependent not only on salinity sources, but also the distribution of salinity across the atmosphere and the volume of air which contains this salinity. It is a reasonable assumption that salinity concentration above the cloud level is negligible and thus salt may distribute from sea level to cloud level. The concentration of salinity thus depends on both transport properties of air and cloud levels. At present we have not been able to incorporate these factors into our model. In order to estimate airborne salinity in the model, it is assumed that each coast type has a maximum airborne salinity (according to Table 1) and that these values are then modified by Eqs (9)–(13).

5.4 Transport of aerosols

Aerosol particles produced by breaking surf tend to be quite coarse (10–50 μm) and are concentrated just above the surf. Particles generated from ocean waves are finer and cover a wider range of sizes (0.5–5 μm). Coarse aerosol particles associated with surf tend to deposit close to the coast, while the finer particles from ocean waves may be carried higher into the atmosphere and deposited further from the coast. In fact, aerosol salt can be distributed up to the cloud layer and may be carried very significant distances, with final deposition be a result of scavenging by rain drops (i.e. salt is deposited by rain). These processes are complex and are being studied by the current authors using CFD and other techniques.

The refined Australian model assumes that the deposition of airborne salinity can be modelled by three terms, i.e. a short- (SRS), a medium- (MRS) and long-range (LRS) term.

The incorporation of salinity sources and distribution mode into the salinity formulation leads to the following definitions:

$$\text{Sal} = [\text{MRS} + \text{LRS} + (\text{SRS} \times \text{s})]/(\text{s} + 1) \quad \textbf{(14)}$$

$$\text{SRS} = \text{PS(W)} \times \text{E} \times e^{(-\text{dist}/\sqrt{\text{s}})} \times \text{CalSRS} \quad \textbf{(15)}$$

$$\text{MRS} = \text{PO} \times [(\text{E} - \text{G}) \times e^{[-\text{dist} \times (\text{s} + 1.5)/275]}] \quad \textbf{(16)}$$

$$\text{LRS} = \text{G} \times e^{(-\text{dist}/\text{H})} \quad \textbf{(17)}$$

where PS(W) is the surf salinity production term derived from Eq. (8), CalSRS is a procedure that equates SRS to zero for coastline adjacent to very sheltered bays, and PO is a term to take into account the variation in salinity produced from the ocean, and is derived from Eqs (10)–(13). The values of G is determined by data fitting to be 5, while H is derived from a combination of data fitting and reference to existing Australian data. Keywood et al. (1997) proposed that the distribution of salinity in rain as a function of distance could be modelled by a sum of two inverse exponential terms (short and long range), with the long range having a decay constant of 600 (in km).

5.5 Effect of winds

In the model outlined in Eqs (14)–(17), “dist” is to a given point on the coast from the point for which the corrosion rate is being determined (the modelled point). The Australian coast is represented by 5000 points and for any modelled point, a radius of influence around the modelled point is defined. This circle is then broken into wind quarters and the average salinity contribution (AvSal) from the coastal points in each quarter is determined according to Eqs (14)–(17). The weighted salinity factor is then given by:

$$\text{Weighted salinity} = \sum \text{AvSal} \times \text{Wind freq} \quad \textbf{(18)}$$

The wind frequency used is that of the modelled point derived from meteorological observations at 3 m elevation. This method permits a consideration of the effect of wind distribution on salinity.

5.6 Accuracy of the Australian model

When the new model is applied to the Australia-wide data, it shows a significant improvement over the South Australian model. In Figure 3 a misfit diagram is presented, and the majority of points (64%) fall between 0.6 and 1.2. The greatest number (19%) of outliers fall between 0.2 and 0.6. Of these, 10% are associated with industrial, 5% with severe marine and 4% with other locations. The model does not as yet account for effects of industrial pollutants, and thus the high misfit is to be expected. Overall the mean average error of the model is 36% and thus the model is reasonably accurate at predicting corrosion across a continent. Further, the errors in the model are now informative and highlight fields in which more work is required.

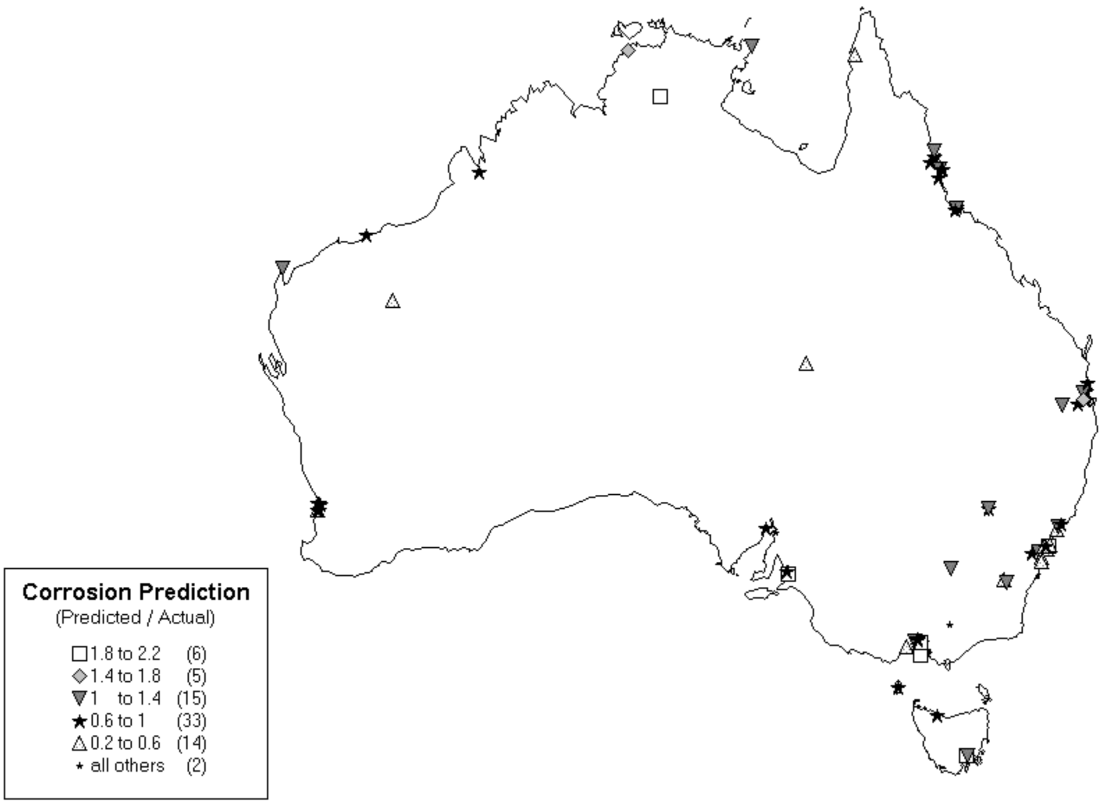

Fig. 3: Misfit diagram for Australian model applied to Australia

6 Conclusions

Two approaches to developing atmospheric corrosion models for regions in Australia have been outlined in this paper. The first is based on regression analysis of large databases of corrosion and climate data, and the second is based on combining such regression analysis with a more detailed modelling of the processes controlling salinity sources and distribution. The following conclusions can be drawn.

- It was found that the regression approach produced models that proved an accurate description of the variation in the data of the databases from which they were constructed. However, these models could not account for the variation observed in a data set derived from a wider range of climates.
- In accounting for corrosion rate across the Australian continent, the role of sea state in controlling salinity production should be considered.
- The use of a salinity distribution term that contains short-, medium- and long-range factors gives rise to satisfactory estimations of corrosion rate.

7 References

Atteraas, L. and Haagenrud, S. (1982) Atmospheric corrosion in Norway. In *Atmospheric Corrosion* (ed. W.H. Ailor), John Wiley & Sons, New York, pp. 873–91.

Benarie, M. and Lipfert, F.L. (1986) A general corrosion function in terms of atmospheric pollutant concentration and rain pH. *Atmospheric Environment*, Vol. 20, No. 10, pp. 1947–58.

Cole, I.S. and Ganther, W. (1996) A preliminary investigation into airborne salinity adjacent to and within the envelope of Australian houses. *Construction and Building Materials*, Vol. 10, No. 3, pp. 203–7.

Egan, F.J. (1971) Effects of environmental factors on the corrosion of steel. *Australian Corrosion Engineering*, Vol. 17, pp. 9–16.

Haynie, F.H. (1982) Evaluation of the effects of microclimate differences on corrosion. In *Atmospheric Corrosion* (ed. W.H. Ailor), John Wiley & Sons, New York, pp. 286–308.

Keywood, M.D., Chivas, A.R., Fifield, L.K., Cresswell, R.G. and Ayers, G.P. (1997) The accession of chloride to the Australian continent. *Australian Journal of Soil Research*, Vol. 35, pp. 1177–89.

King, G.A. (1993) Corrosivity mapping – a sensitive and cost-effective means of characterising a region's level of atmospheric corrosion. Proc. Corrosion 93, NACE, New Orleans, USA, 7–12 March 1993, Paper No. 638.

Martin, K.G. (1973) Atmospheric corrosion of metal cladding in Papua New Guinea and Melbourne. *Australian Corrosion Engineering*, Vol. 19, pp. 19–27.

Martin, K.G., and King, G.A. (1981) Corrosivity measurements at some Australian cities. *Corrosion Australasia*, Vol. 6, No. 4, pp. 10–6.

McKay, W.A., Garland, J.A., Livesley, D., Halliwell, C.M. and Walker, M.I. (1994) The characteristics of the shoreline sea spray and the landward transfer of radionuclides discharged to coastal sea water. *Atmospheric Environment*, Vol. 28, pp. 3299–309.

Monahan, E.C. (1980) Positive charge flux from the world oceans resulting from the bursting of white cap bubbles. Proc. VI Int. Conf. on Atmospheric Chemistry, Manchester, UK, pp. 147–50.

Monahan, E.C, Davidson, K.L. and Spiel, D.E. (1982) Whitecap aerosol productivity deduced from simulation tank measurements. *Journal of Geophysical Research*, Vol. 87, pp. 8898–904.

Monahan, E.C., Spiel, D.E. and Davidson, K.L. (1986) A model of marine aerosol generation via whitecaps and wave disruption. In *Oceonic Whitecaps* (eds E.C. Monahan and G. Macnioaill), D. Reidel Publishing Company, pp. 167–74.

Okabe, A., Boots, B. and Suguhara, H. (1992) *Spatial Tessallations: Concepts and Applications of Voronoi Diagrams*. John Wiley & Sons, New York.

Smith, B.S., Duxbury, E.J. and Moore, B.T. (1994) *Atmospheric Corrosivity of Defence Bases in Northern and Eastern Australia*. Technical Report DSTO-GD-0123. Department of Defence, Australia.

Spence, J.W. and Haynie, F.H. (1990) Derivation of a damage function for galvanised steel structures: corrosion kinetics and thermodynamic considerations. In *Corrosion Testing and Evaluation: Silver Anniversary Volume*, ASTM STP 1000, pp. 208–24.